AN EXPLICIT, NON-ITERATIVE, SINGLE EQUATION FORMULATION FOR AN ACCURATE ONE DIMENSIONAL ESTIMATION OF VANELESS RADIAL DIFFUSERS IN TURBOMACHINES

R. Amirante * **F. De Bellis** **E. Distaso** **P. Tamburrano**

Department of Mechanic Mathematic and Management
Polytechnic University of Bari
Bari, Italy

ABSTRACT

The present paper proposes a very simple one dimensional (1-D) model that accounts for the energy loss caused by the fluid dynamic losses occurring in the vaneless diffusers of centrifugal compressors and pumps. Usually, the present techniques to design turbomachines (pumps, compressors and turbines) emphasize numerical methods and their use is relatively complex because several parameters need to be chosen and a lot of time is required to perform the calculation. For this reason, it is relevant to perform an accurate preliminary design to simplify the numerical computation phase and to choose a very good initial geometry to be used for accelerating and improving the search for the definitive geometry. However, today 1-D modeling is based on the classical theory that assumes that the angular momentum is conserved inside a vaneless diffuser, although the flow evolution is considered as non-isentropic. This means that fluid-dynamic losses are taken into account only for what concerns pressure recovery, whereas the evaluation of the outlet tangential velocity incoherently follows an ideal behavior. Starting from such considerations, a new conservation law for the angular momentum is analytically derived, which incorporates the same fluid-dynamic losses modeled by the thermodynamic transformation law that is employed for correlating pressure recovery with enthalpy increase. Similar arguments hold for incompressible flows. Detailed and very accurate three-dimensional flow simulations are employed to analyze if the new model is capable of predicting the outlet tangential velocity more accurately than the classical theory. Results provided for both compressible (centrifugal compressors) and incompressible (centrifugal pumps) flows and for different inlet velocity profiles show a significant accuracy improvement of the new conservation law in the prediction of the outlet flow conditions when compared with the classical theory, thus demonstrating that the proposed model can be employed in the preliminary design of vaneless diffusers (*i.e.*, in the estimation of the outlet diameter) more effectively than the classical ideal theory. Furthermore, the model is validated against industrial experimental campaigns. Even further experimental data, reported in a previous paper by the same authors, confirm the reliability of the employed approach.

Keywords: Energy loss, Turbomachinery efficiency, Centrifugal compressor and pump, Vaneless diffuser.

1. INTRODUCTION

Since 1970 the energy loss calculation in diffusers of centrifugal pumps and centrifugal compressors has been one of the most important topics for industrial and university researchers [1]. The efficiency improvement of turbomachines is a great challenge to obtain higher performance of industrial plants and of automotive engines because their application is widely used. A large number of patents, aiming to reduce the length of components and thereby pressure losses, have already been filed for the last twenty years [1-3]. Furthermore, experimental setup have been carried out to evaluate interaction between rotor and stator in steady and unsteady conditions [4]. More recently some authors have tried to improve the prediction of the complex, three-dimensional, unsteady flow associated with the interaction between a centrifugal impeller and its vaned diffuser, in an attempt to find the optimum loss models for performance prediction [5,6]. Current research on modeling and experimenting diffusers for centrifugal turbomachines mainly deals with three–dimensional and unsteady aspects of their operation [7,8] which affect boundary layer development and thus their performance. Some authors propose efficient algorithms based on gradient-based progressive optimization techniques, which can efficiently be combined with black-box simulation codes to design the intake section of diffusers [9]. Like a full 3D model that was successfully utilized by the same authors of this paper to automatically optimize valves performances [10], each of these techniques requires great employment of compu-

* Corresponding author (amirante@poliba.it)

DOI : 10.1017/jmech.2014.72
Copyright © 2014 The Society of Theoretical and Applied Mechanics, R.O.C.
https://doi.org/10.1017/jmech.2014.72 Published online by Cambridge University Press

tational time. In contrast the (preliminary) design of this crucial component of centrifugal compressors and, when present, of centrifugal pumps, is based on a simple two-dimensional model, as shown in many manuals [11,12]. For vaneless radial diffusers, continuity is combined with the assumption of constant angular momentum to model the evolution of radial and tangential components of velocity. The above assumption considers the flow isentropic, that is, all fluid-dynamic losses are discarded when calculating the variations of the tangential velocity. In contrast, pressure losses are included when evaluating how much kinetic energy is converted into pressure by using experimental correlations widely available in the scientific and technical literature. For example, Lakshminarayna [12] and Turton [13] show the performance of the vaneless diffuser in terms of ratio of actual to ideal pressure rise for some given geometries. It is noteworthy that these correlations are useful to evaluate pressure losses, but not velocity losses.

The above procedure, reported in books and manuals and usually employed for designing the outlet diameter, appears to be inconsistent, since pressure losses are included in one equation only. More importantly, discarding angular momentum losses leads to a theoretical higher velocity at the outlet of the diffuser and thus to designing a longer (and bulkier) diffuser. Finally, it should be pointed out that the overestimation of the outlet tangential velocity also introduces significant errors in the design of the downstream component, namely the volute. To the authors' knowledge, the unique attempt to include pressure losses also in the equation of the angular momentum is reported by Gulich in his fundamental book on centrifugal pumps [13]. The proposed relationship, taken from Pfleiderer [14], is strictly valid for incompressible flows only and requires the evaluation of the friction coefficient f for calculating the angular momentum loss ΔAM:

$$\Delta AM = \frac{2\, f\, R_2}{\delta \sin\alpha_{2'} \cos\alpha_{2'}^{\,2}} \left(\frac{c_{u2}}{u_2}\right)^2 \left(1 - \frac{R_2}{R_3}\right)$$

where subscripts 2, 2' and 3 denote the impeller exit, the diffuser inlet and the diffuser outlet, respectively, c_u is the tangential component of the absolute velocity, R is the radius, δ is the diffuser width, u is the tangential velocity of the impeller and α is the angle between the absolute velocity and the tangential direction. In the case of centrifugal compressors, Ludtke [15] suggests the presence of a friction correction F_r, but without proposing any numerical evaluation of it:

$$c_{u3} = \frac{R_{2'}}{R_3} c_{u2'} - F_r$$

Discarding angular momentum losses leads to a higher theoretical velocity at the diffuser outlet and thus to a different exit flow angle.

Therefore, if accurate predictions are needed, the hypothesis of constant angular momentum must necessarily be rejected. This paper proposes how to remove inconsistency in the two-dimensional modeling of a radial vaneless diffuser, by deriving a new equation for the angular momentum, which does take dissipation effects into account. The developed equation is valid both for compressible and for incompressible flows; moreover, it does not require the knowledge of any other loss coefficient such as the one already employed in the equation describing conversion of kinetic energy into pressure.

The next section will describe the mathematical derivation of the new model in detail. Then, its improved accuracy will be assessed by means of steady-state, grid-converged, numerical simulations of a radial vaneless diffuser; a grid-convergence study and a preliminary choice of the turbulence model, which were performed in order to determine the most suitable simulation setting, will also be described; after that, the results of the CFD simulations of both compressible and incompressible flows, with two different inlet velocity profiles, will be presented and critically discussed. The computed flow field, along with data of an extensive experimental campaign, will finally be used to verify the accuracy improvement of the proposed theory.

2. NEW MODEL INCLUDING ANGULAR MOMENTUM LOSS

The classical theory, describing how a vaneless radial diffuser converts kinetic energy into pressure, is based on a two-dimensional approach [10,11], and neglects blade wakes and leakage. Making reference to the compressible flow case, mass flow conservation between the inlet and the outlet sections of the diffuser, denoted by 2 and 3 respectively, results in

$$\pi D_2\, c_2 \sin\alpha_2\, \rho_2 = \pi D_3\, c_3 \sin\alpha_3 \rho_3 \; ; \qquad (1)$$

having assumed that the diffuser has constant width, δ, as usual. In Eq. (1), D_2 ($D_{2'} \cong D_2$) and D_3 represent the inlet and the outlet diameters, whereas the corresponding absolute values of the velocity vectors, forming the angles α_2 and α_3 with the tangential direction, are denoted by c_2 and c_3, and ρ is the fluid density.

In the classical theoretical approach, it is assumed that angular momentum is conserved in a vaneless diffuser. This means that any dissipation determined by the fluid-dynamic losses is neglected, which leads to

$$D_2 c_2 \cos\alpha_2 = D_3 c_3 \cos\alpha_3 \; . \qquad (2)$$

In contrast, the transformation law that correlates the thermodynamic properties in 2 and 3 usually incorporates losses, *e.g.* by means of the polytropic efficiency:

$$\frac{T3}{T2} = \left(\frac{p_3}{p_2}\right)^{\frac{\gamma-1}{\gamma \eta_p}} \; . \qquad (3)$$

Equations (1) and (2) describe the diffusion of the velocity, for its radial and tangential components respectively; they are usually used in combination with

https://doi.org/10.1017/jmech.2014.72 Published online by Cambridge University Press

Eq. (3) for the preliminary design of a vaneless diffuser of a centrifugal compressor, namely for the evaluation of the outlet diameter D_3 that allows a prescribed pressure recovery to be performed. Since the tangential component of the velocity contributes to the kinetic energy for almost its 90%, its evolution needs to be properly described.

The following analytical development aims at incorporating real effects and fluid-dynamic losses also in the conservation of the angular momentum, by employing the same parameters already used in the other equations, *i.e.* Eqs. (1) and (3), namely without introducing any other parameter requiring experimental correlations.

As usual, blade wakes can be taken into account by introducing one coefficient into the left hand side of Eq. (1), namely wake coefficient ξ, lower than unity:

$$\xi D_2 c_2 \sin\alpha_2 \rho_2 = D_3 c_3 \sin\alpha_3 \rho_3 . \tag{4}$$

Fluid-dynamic losses not only influence the pressure recovery, namely the transformation of kinetic energy into pressure (see Eq. 3), but also determine a reduction in the angular momentum ΔAM. This loss needs to be taken into account in the corresponding conservation equation, both for consistency and for improving the accuracy of this 1-D model, *e.g.* in evaluating D_3 during the preliminary design of a diffuser:

$$\frac{D_2}{2} c_2 \cos\alpha_2 = \frac{D_3}{2} c_3 \cos\alpha_3 + \Delta AM . \tag{5}$$

Equation (5) can also be written in terms of a percentage reduction in the angular momentum as

$$\frac{D_2}{2} c_2 \cos\alpha_2 (1 - k_{\Delta AM}) = \frac{D_3}{2} c_3 \cos\alpha_3 . \tag{6}$$

Examination of Eqs. (4) and (5) reveals that the radial and tangential components of the outlet velocity are less than those calculated by the classic model.

With the aim to produce a more accurate and complete formulation of the momentum conservation in the diffuser, which even maintains the overall design structure and simplicity of the ideal case, it is chosen to maintain the classical approach assumption [9]:

$$\alpha_2 \approx \alpha_3 . \tag{7}$$

which, combining Eqs. (4) and (6), leads to

$$\frac{\rho_3}{\rho_2 \xi} (1 - k_{\Delta AM}) = 1 , \tag{8}$$

As a consequence of Eq. (7) we assume a constant flow angle α and then the angular momentum loss ΔAM can be derived by integrating the moment of the elementary friction forces $\tau_w dS$, according to the streamline, over each of the two diffuser surfaces, $S_d = \pi(R_3^2 - R_2^2)$, with R denoting the radius:

$$\Delta AM = \frac{\int_{S_d} 2\tau_w R \cos\alpha dS}{\dot{m}} . \tag{9}$$

where τ_w is the wall shear stress along the flow path and $\dot{m}$ is the mass flow rate. Calculating τ_w as

$$\tau_w = \frac{1}{8} f \rho c^2 \tag{10}$$

and considering a circular area element $dS = 2\pi R dR$, one gets:

$$\Delta AM = \frac{\int_{R_2}^{R_3} 2 \times \frac{1}{8} f \rho c^2 \times R \cos\alpha \times 2\pi R dR}{\dot{m}} . \tag{11}$$

Note that both f and cR do not undergo any significant change within the diffuser and indeed the term cR is exactly constant in the ideal case, therefore it is also reasonable to consider the whole integrand $f c^2 R^2$ almost constant and to get it out from the integral. Furthermore, in order to be able to analytically solve the integral of Eq. (11), we consider an appropriate average value of the density ρ. Let $\bar{\rho}$ and $\overline{f c^2 R^2}$ be the average values of the corresponding variables, we can write Eq. (11) as follows

$$\Delta AM = \frac{\frac{\pi}{2} \bar{\rho} \cos\alpha \, \overline{f c^2 R^2} \, (R_3 - R_2)}{\dot{m}} . \tag{12}$$

The work done by the friction forces, denoted by W_f, is related, similarly to ΔAM, to the wall shear stress. Considering an elementary mass between the two walls of the diffuser, $dm = \rho \cdot \delta dS$, which carries out an infinitesimal displacement ds, it undergoes an infinitesimal friction work

$$dW_f = \frac{2\tau_w \, dS ds}{\rho \delta dS} = \frac{2\tau_w \, ds}{\rho \delta} . \tag{13}$$

Integrating the last equation along the entire flow path, of length Δs, one has:

$$W_f = \frac{2}{\delta} \int_{\Delta s} \frac{\tau_w}{\rho} \, ds . \tag{14}$$

Considering $ds = dR/\sin\alpha$ and using Eq. (10), Eq. (14) becomes:

$$W_f = \frac{2}{\delta} \int_{R_2}^{R_3} \frac{1}{8} f c^2 \frac{dR}{\sin\alpha} .$$

Taking the average value $\overline{f c^2 R^2}$ out of the integral and confusing it with the average value employed in Eq. (12), considering that the averaging procedures are different, one obtains

$$W_f = \frac{\overline{f c^2 R^2}}{4\delta \sin\alpha} \int_{R_2}^{R_3} \frac{dR}{R^2} = \frac{\overline{f c^2 R^2}}{4\delta \sin\alpha} \left[-\frac{1}{R} \right]_{R_2}^{R_3} ,$$

and finally

https://doi.org/10.1017/jmech.2014.72 Published online by Cambridge University Press

$$W_f = \frac{\overline{fc^2R^2}(\mathrm{R}_3 - \mathrm{R}_2)}{4\delta R_2 R_3 \sin\alpha}. \tag{15}$$

Rearranging Eq. (15) as follows

$$\overline{fc^2R^2}(\mathrm{R}_3 - \mathrm{R}_2) = 4W_f\,\delta R_2 R_3 \sin\alpha\,.$$

and using Eq. (12), the loss of angular momentum, ΔAM, can be expressed as a function of W_f:

$$\Delta AM = \frac{\frac{\pi}{2}\overline{\rho}\cos\alpha 4W_f\,\delta R_2 R_3 \sin\alpha}{\dot{m}}. \tag{16}$$

Since $\dot{m} = \xi\pi D_2 \delta\rho_2 c_{u2}\tan\alpha_2$, where c_{u2} is the tangential component of the absolute velocity, and having assumed $\rho \approx$ cost, *e.g.* $\overline{\rho} = \rho_2$, one gets:

$$\Delta AM = \frac{\frac{\pi}{2}\cos\alpha\ 4W_f \delta R_2 R_3 \sin\alpha}{\xi\pi D_2\,\delta c_{u2}\dfrac{\sin\alpha_2}{\cos\alpha_2}}. \tag{17}$$

Substituting ΔAM of Eq. (17) into Eq. (5) and assuming $\cos\alpha = \cos\alpha_3$ and $\sin\alpha = \sin\alpha_2$ since $\alpha_2 = \alpha_3 = \alpha$ (Eq. (8)), one obtains

$$D_2 c_{u2} - D_3 c_{u3} = \frac{\cos\alpha_3 \cos\alpha_2 W_f D_3}{\xi c_{u2}}. \tag{18}$$

After a few steps, one finally gets

$$D_2 c_{u2} = D_3 c_{u3}\left(1 + \frac{W_f}{\xi c_2 c_3}\right). \tag{19}$$

Equation (19) represents a consistent, more accurate and very simple one dimensional (1-D) model to express conservation law for the angular momentum, which can simply substitute Eq. (2) in the standard two-dimensional modeling of a vaneless diffuser: indeed, Eq. (19) considers the loss of angular momentum caused by friction forces as a simple function of the corresponding dissipation work W_f. It is noteworthy that W_f can be retrieved by the polytropic efficiency η_p, which is already employed to evaluate the pressure recovery (see, *e.g.*, Eq. (3) for the case of a compressor diffuser) and can be obtained from the available experimental correlations cited in the Introduction.

3. COMPUTATIONAL FLUID DYNAMIC EVALUATION

A very accurate, three-dimensional, steady-state Navier-Stokes computation of the compressible and of the incompressible flow inside a vaneless radial diffuser are proposed in this section, with the aim of validating the consistent conservation equation of the angular momentum developed so far. In fact, the numerical computations are capable of predicting the real values of the flow variables and the diffuser efficiency. Since both the proposed new model and the classical one neglect the unsteadiness induced by the impeller, steady inlet conditions were considered in the simulations. In particular, the numerical simulations were used to compute the mass-averaged values and the outlet velocity c_3. Its tangential component c_{u3} was compared with the one prescribed by the classical theory, Eq. (2),

$$c_{u3,\mathrm{id}} = c_{u2}\frac{D_2}{D_3}, \tag{20}$$

and with the one resulting from the application of the proposed new Eq. (19), in which the wake coefficient ξ is set equal to unity to allow the comparison:

$$c_{u3,\mathrm{wf}} = c_{u2}\frac{D_2}{D_3}\frac{1}{\left(1 + \dfrac{W_f}{c_2 c_3}\right)} \tag{21}$$

namely

$$c_{u3,\mathrm{wf}} = c_{u3,\mathrm{id}}\left(1 - \frac{W_f}{W_f + c_2 c_3}\right). \tag{22}$$

The dissipation work W_f was computed using the well-known equation that combines the first and the second principles of the thermodynamics in the following manner

$$W_f = R'\frac{\gamma\eta_p}{\gamma - 1}(T_2 - T_3) + \frac{c_2^2 - c_3^2}{2}, \tag{23}$$

for the compressible flow case, and

$$W_f = \frac{p_2 - p_3}{\rho} + \frac{c_2^2 - c_3^2}{2}, \tag{24}$$

for the incompressible one. As obvious, p_3 and T_3 are the (mass-averaged) real values of outlet pressure and temperature resulting from the numerical simulations, and the polytropic efficiency η_p was computed using Eq. (3). The percentage deviation from the real value of c_{u3} can be defined for each of the two predicted outlet tangential velocities as

$$s\%(c_{u3,\mathrm{id}}) = \frac{c_{u3,\mathrm{id}} - c_{u3}}{c_{u3}}100 \tag{25}$$

and

$$s\%(c_{u3,\mathrm{wf}}) = \frac{c_{u3,\mathrm{wf}} - c_{u3}}{c_{u3}}100, \tag{26}$$

respectively.

A vaneless diffuser with an outlet radius double than the inlet radius was considered: its geometrical data are reported in Table 1, where, again, subscript 2 refers to diffuser inlet conditions and subscript 3 to outlet conditions. Given the axisymmetric nature of the computational domain, only one eighth of the diffuser was modeled in order to reduce the mesh size and thus the computational time. With reference to Fig. 1, the bottom

https://doi.org/10.1017/jmech.2014.72 Published online by Cambridge University Press

Table 1 Diffuser geometry.

Parameter	Dimension
D_2	400mm
D_3	800mm
δ	17mm

surface is the diffuser solid wall, the violet surface is the flow inlet, the red surface is the flow outlet, whilst the lateral surfaces are considered as rotational periodic boundaries and the upper surface as a symmetry boundary.

The flow was modeled as a steady, compressible ideal gas, whilst a second order discretization was used for all the equations. Flow turbulence was modeled by means of the Reynolds Averaged Navier Stokes (RANS) approach; the commercial CFD package ANSYS Fluent was employed [16].

Concerning the boundary conditions, the value of total pressure p_2^0 was imposed at the inlet, while static pressure was assigned at the outlet. Believing reasonable, for the given geometry, to assume $c_{u2} = 257.4$m/s, $\alpha_2 = 18.5°$, $p_2 = 2$bar and $T_2 = 350$ K, the value of the total pressure p_2^0 at the diffuser inlet resulting from these assumptions is 2.83bar. The outlet static pressure was set equal to 2.6bar (to avoid a too high adverse pressure gradient).

Since a detailed boundary layer was required, the inlet velocity was analytically defined by using the 1/7th-power velocity-distribution law to compute the velocity profile in the boundary layer. The equation was proposed by Hermann Schlichting [17] as follows:

$$\frac{u(z)}{U_0} = \left(\frac{z}{\delta_{BL}}\right)^{\frac{1}{7}}, \tag{27}$$

where U_0 is the constant undisturbed velocity outside the boundary layer (corresponding to absolute velocity c_2) and δ_{BL} is the boundary layer height, quantified by the empirical relation derived by Schlichting [17]:

$$\frac{\delta_{BL}}{l} = \frac{5}{\sqrt{Re}} \rightarrow \delta_{BL} = 5\sqrt{\frac{\nu l}{U_0}}, \tag{28}$$

where v is the air kinematic viscosity and l is the height of the computational domain. Having assumed $v = 20.76e^{-6}$m^2/s and l equal to one half of the diffuser width, the resulting boundary layer height is:

$$\delta_{BL} = 0.1561 \text{ mm}. \tag{29}$$

However, for a compressible flow, inlet boundary conditions require the definition of the total pressure instead of the absolute velocity (the angle with the tangential direction was only imposed: $\alpha_2 = 18.5°$); as a consequence, the Mach number was calculated as follows:

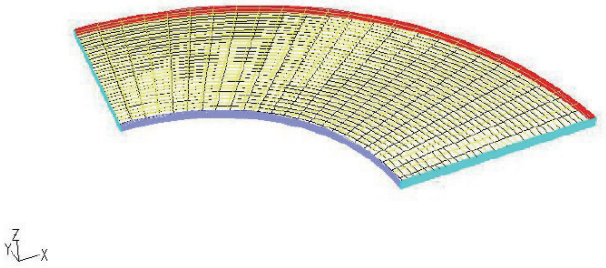


Fig. 1 Computational domain.

$$Ma_2(z) = \frac{u(z)}{\sqrt{\gamma R' T_2}}, \tag{30}$$

then the total pressure distribution was obtained and it was imposed at the entrance of the diffuser:

$$p_2^0(z) = p_2\left[1 + \frac{\gamma - 1}{2}\left(Ma_2(z)\right)^2\right]^{\frac{\gamma}{\gamma-1}}. \tag{31}$$

Figure 2 shows the total pressure distribution at diffuser inlet, obtained by (31).

Since CFD results are considered the benchmark in the present study, an appropriate computational grid had to be generated. To that end, a grid-convergence study was initially arranged with seven different meshes, with increasing number of cells, as reported in Table 2. Note that the ratio between two subsequent cells height was kept constant in all of the meshes.

In order to verify the independence of the results from the grid size, some relevant fluid-dynamics quantities such as velocity and pressure were compared for the seven different meshes. For grid study purposes, the Standard k-ε was selected, with the Enhanced Wall Treatment option (boundary layer refinement corresponding to $y^+ \approx 1$); turbulence intensity was set equal to 5% and turbulent length scale to 10^{-3}m. The quantities were mass averaged (for this analysis and the following ones); denoting the generic quantity by v, one gets

$$\overline{v} = \frac{\sum_{i=1}^{n} v_i \dot{m}_i}{\sum_{i=1}^{n} \dot{m}_i}, \tag{32}$$

where n is the number of cells on surface A where the average is calculated. The previous equation can also be written as:

$$\overline{v} = \frac{\int_A \rho c_r \, v \, dA}{\int_A \rho c_r \, dA}. \tag{33}$$

In Table 3 the values of pressure and absolute velocity at the diffuser inlet are reported together with the percentage difference of the values obtained on two consecutive grids. These values clearly indicate that the inlet conditions are sufficiently independent of the mesh size for the finer grids.

https://doi.org/10.1017/jmech.2014.72 Published online by Cambridge University Press

Although the quantities in Table 3 differ from the values computed on the immediately coarser mesh of 0. 1% or less, already at the grid level 4, the finest grid (*i.e.*: 7) was chosen and employed in the other calculations. Note that the percentage difference between consecutive grids was calculated as follows:

$$err(\overline{v}) = 1 - \frac{\overline{v}_{grid,i}}{\overline{v}_{grid,i+1}}.$$

Table 4 shows how the grid size influences the outlet conditions and, in particular, the percentage deviation of the calculated tangential velocity from the corresponding CFD prediction. The tangential velocities

Table 2 Number of cells employed in the grid study.

Grid	Axial	Radial	Circumferential	total
1	32	32	24	24576
2	40	40	30	48000
3	50	50	38	95000
4	64	64	46	188416
5	86	86	52	384592
6	108	108	66	769824
7	136	136	83	1535168

Table 3 Mass flow averaged values at diffuser inlet and percentage differences between consecutive grids.

Grid	$\overline{c_2}$[m/ s]	$\overline{p_2}[Pa]$	$d\%(\overline{c_2})$	$d\%(\overline{p_2})$
1	229.99	220929	/	/
2	231.77	220093	0.764	0.380
3	232.24	219872	0.203	0.101
4	232.48	219761	0.103	0.051
5	232.66	219674	0.081	0.039
6	232.74	219638	0.036	0.016
7	232.81	219613	0.026	0.011

are calculated by the classical theory and by the model proposed in this paper, and their percentage deviations from CFD values are denoted by $s\%(c_{u3,id})$ and $s\%(c_{u3,Wf})$, respectively (see Eqs. 25 and 26).

Table 4 clearly demonstrates the significant improvement in predicting the outlet tangential velocity. The same results are also plotted in Fig. 3, highlighting that the difference due to the increasing number of cells is much less pronounced than the one existing between the proposed model and the "classical" theory. In fact, the maximum difference between the coarsest and the finest grid is about 2% for both models, whilst the proposed new model shows an improved estimation of outlet velocity of an order of magnitude for all grids (when compared with CFD), thus giving a more realistic description of the physical flow evolution inside the diffuser.

After the grid-convergence study had been performed, it was still a matter of concern if the results were somehow affected by the turbulence model; in other words, a quantification of the error introduced by the turbulence model was still needed. This task was faced by repeating the abovementioned analyses using the finest grid and two additional RANS turbulence models, namely the Spalart-Almaras and the *k*-ω, in addition to the already used *k*-ε model.

The results of such a comparison are reported in Table 5, which provides the outlet tangential velocity obtained by using the three turbulence models and by using the two analytical theories (using again Eqs. (20) and (22)); the percentage deviations from CFD are enclosed in Table 6, similarly to the previous analysis.

Also in this case a plot of the percentage deviations (see Fig. 4) helps to understand the effect of the turbulence model on the results: again, the difference between the two analytical models is much more significant than the variation due to the change of turbulence model. In particular, the negative sign indicates that the proposed non-isentropic model slightly overestimates the losses in the diffuser, whilst the "classical" isentropic assumption leads to a noticeable losses underestimation (or outlet velocity overestimation), as expected.

A more realistic model of the diffuser operation can be obtained by improving the diffuser inlet flow conditions. Up to now, the flow entering the diffuser has been described only by the $1/7^{th}$-power velocity-distribution law applied to the absolute velocity along the axial direction. However, in real operating conditions, only the relative velocity at the impeller exit, w_2, reduces down to zero at wall; the difference can be noticed in Fig. 5. It should be noted that, since c_2 is the vector sum of w_2 and the constant u_2 (tangential velocity at impeller outlet), an axial variation in the relative velocity w_2 also means a variation in the direction of absolute velocity c_2, and not only in its modulus.

Table 4 Percentage deviation of outlet tangential velocity, calculated by the two models, from CFD.

Grid	$s\%(c_{u3,id})$	$s\%(c_{u3,Wf})$
1	11.45	-2.85
2	11.52	-2.46
3	12.08	-2.12
4	12.63	-1.83
5	13.16	-1.56
6	13.48	-1.41
7	13.75	-1.21

https://doi.org/10.1017/jmech.2014.72 Published online by Cambridge University Press

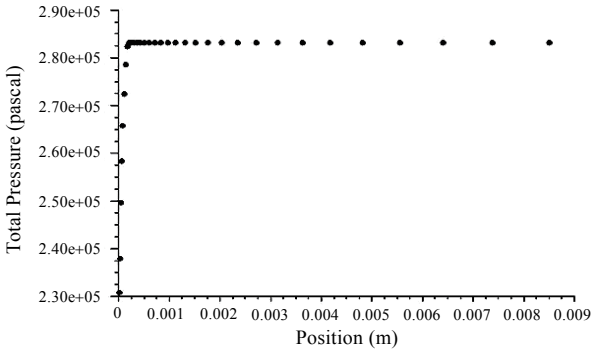


Fig. 2 Total pressure distribution imposed at the diffuser inlet.

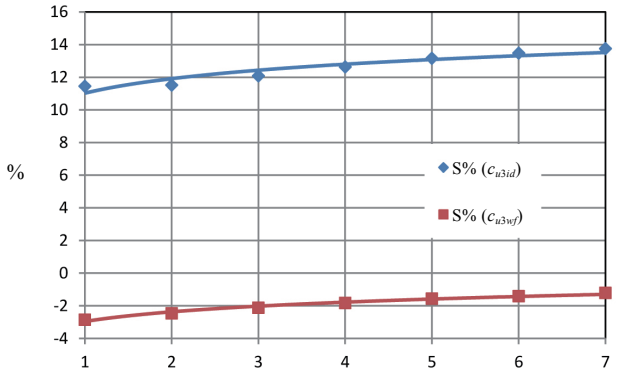


Fig. 3 Percentage deviation of $s\%(c_{u3,id})$ and $s\%(c_{u3,Wf})$ versus grid variation.

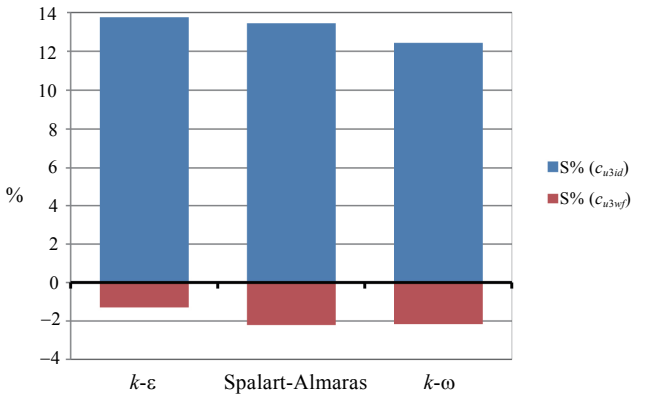


Fig. 4 Turbulence model and analytical theories influence.

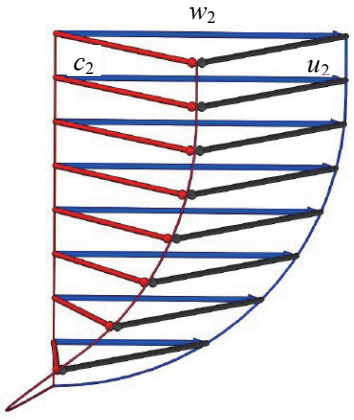


Fig. 5 Skewed profile.

Table 5 c_{u3} values calculated by the analytical theories and compared with CFD.

Turbulence model	$c_{u3,CFD}$ [m/s]	$c_{u3,id}$ [m/s]	$c_{u3,Wf}$ [m/s]
k-ε	96.624	109.91	95.714
Spalart-Almaras	95.300	108.11	93.196
k-ω	96.998	109.06	94.904

Table 6 Percentage deviation of outlet tangential velocity depending on the turbulence model.

Turbulence model	$s\%(c_{u3,id})$	$s\%(c_{u3,Wf})$
k-ε	13.75	–1.29
Spalart-Almaras	13.44	–2.21
k-ω	12.43	–2.16

The resulting variation in the boundary layer region is three-dimensional and it was considered in the boundary condition at the diffuser inlet by assuming the angle at which the relative fluid leaves the impeller constant and equal to 70°. The 1/7[th]-power velocity-distribution law was first applied to w_2:

$$w_2(z) = w_{20}\left(\frac{z}{\delta_{BL}}\right)^{\frac{1}{7}}; \tag{34}$$

then, c_2 was obtained as

$$\boldsymbol{c}_2(z)|_{z_i} = (\boldsymbol{w}_2|_{z_i} + \boldsymbol{u}_2)\left(\frac{z}{\delta_{BL}}\right)^{\frac{1}{7}}. \tag{35}$$

The CFD calculations for the present case were obtained with the k-ε turbulence model. Table 7 compares the results obtained by the two analytical models against the data derived from the CFD computations, whilst Table 8 highlights the influence of using the skewed profile or not (boundary layer profile applied to w_2 or directly to c_2, respectively). Both Tables indicate that the effectiveness of the proposed model is not affected by the employment of a more complex (and more realistic) inlet velocity profile.

The proposed model for angular momentum conservation was applied to incompressible flows as well (water). In the latter case, the friction work W_f can easily be estimated by means of the generalized Bernoulli equation between diffuser inlet and outlet, neglecting geodetic difference, see Eq. (24).

Boundary layer height was recalculated: being $v = 1.12e^{-6}\text{m}^2/\text{s}$ the kinematic viscosity of water at 15.6°C, the new value is:

$$\delta_{BL} = 0.01260\text{mm}. \tag{36}$$

https://doi.org/10.1017/jmech.2014.72 Published online by Cambridge University Press

With the same grid used for the previous analyses and the k-ε turbulence model, the tangential velocities at diffuser outlet contained in Table 9 were obtained (with imposed velocity inlet due to incompressible flow formulation, reported for completeness), whilst Table 10 compares the values obtained with the two theories (Eqs. (20) and (22)) and the one extracted from CFD computations. Looking at the percentage deviations displayed in Table 11, there is evidence that the order of magnitude difference between the "classical" isentropic theory and the proposed model is confirmed also in the incompressible flow case.

4. EXPERIMENTAL VALIDATION

The proposed model was validated against experimental data of extensive test campaigns, including variation in both diffuser geometries and operating conditions. Table 12 shows the very large number of tests that were considered, for a total of more than 1000 different experimental datasets divided into 6 test campaigns. A more detailed and complete description of both this experimental campaign and the experimental devices can be found in a recent study by the same authors [17], to which the reader is referred for further deepening on the results hereinafter exposed.

In order to assess the accuracy of the proposed method, the tangential component of the velocity at the diffuser exit was first calculated by using Eq. (21) and then compared with the corresponding measured value of each test point. In particular, the dissipated work was calculated by applying the first principle of thermodynamics between diffuser inlet and outlet, as previously done for the numerical evaluation (Eq. (23)), and by using the values of pressure, temperature and velocity obtained from the experimental measurements. Nevertheless, any other available calculation method could be used for the prediction of W_f for a given diffuser geometry and fixed inlet conditions.

Table 13 shows that the tangential velocities calculated by the proposed model are in good agreement with the experimental data; the comparison with the classical theory (ideal behavior, Eq. (20)) is also shown. It is noteworthy that the assumption of an ideal behavior in the diffuser produces an over-prediction of the tangential velocity in all test campaigns, *i.e.* for different stage designs and diffuser geometries. The average over-prediction is more than 6% and was anyway expected, see Eq. (6). In contrast, the proposed model has shown a better agreement both in terms of accuracy and precision and in general a slight under-prediction of the tangential velocity was observed when employing the proposed model [18]. The overall average deviation of the proposed model from the measurements is less than 3% (Table 13), providing a reliable validation for the proposed model.

Table 7 c_{u3} values calculated by the analytical theories and compared with CFD with the skewed profile.

Turbulence model	$c_{u3,CFD}$ [m/s]	$c_{u3,id}$ [m/s]	$c_{u3,Wf}$ [m/s]
k-ε	96.642	109.95	95.395

Table 8 Percentage deviations with and without the skewed profile.

	Turbulence model	$s\%(c_{u3,id})$	$s\%(c_{u3,Wf})$
Skewed profile	k-ε	13.78	-1.2905
c_2 profile	k-ε	13.75	-1.2902

Table 9 Mass flow averaged values for incompressible flow.

Turbulence model	c_{u2} [m/s]	c_{u3} [m/s]	c_2 [m/s]	c_3 [m/s]
k-ε	28.443	12.533	29.996	13.487

Table 10 c_{u3} values calculated by analytical theories and compared with CFD considering an incompressible flow.

Turbulence model	$c_{u3,CFD}$ [m/s]	$c_{u3,id}$ [m/s]	$c_{u3,Wf}$ [m/s]
k-ε	12.533	14.222	12.375

Table 11 Percentage deviations from CFD considering an incompressible flow.

Turbulence model	$s\%(c_{u3,id})$	$s\%(c_{u3,Wf})$
k-ε	13.48	–1.2581

Table 12 Test campaigns specifications.

Test	R_3 / R_2	$1 / R_2$	$n°$ points
1	1.350	0.067	80
2	1.350	0.051	76
3	1.350	0.048	226
4	1.280	0.072	211
5	1.280	0.094	57
6	1.280	0.081	64

https://doi.org/10.1017/jmech.2014.72 Published online by Cambridge University Press

Table 13 Results summary in terms of deviation error of the classical theory and the proposed model from experimental data of the modulus of the tangential velocity at the diffuser exit.

Test	Classical Theory		Proposed Model	
	Average [%]	Standard deviation [%]	Average [%]	Standard deviation [%]
1	10.6	8.1	–1.1	4.0
2	15.7	4.9	0.8	3.4
3	8.6	4.5	–2.5	1.7
4	6.3	6.2	–3.0	2.4
5	5.5	4.5	–2.1	1.0
6	3.4	1.7	–2.8	0.5
Overall	6.3	6.4	–2.8	2.7

5. CONCLUSIONS

To perform an accurate preliminary design and simplify the numerical computation phase, the authors proposed a very simple one dimensional (1-D) model that accounts for the energy loss caused by the fluid dynamic losses occurring in vaneless diffusers of centrifugal compressors and pumps. A new equation describing the evolution of the tangential velocity in a vaneless radial diffuser was derived. It was demonstrated that the developed model is valid for both compressible and incompressible flows and requires no additional information with respect to the classical theory. The new equation takes the friction effects into account, which are usually considered only in the pressure recovery equation: thus, it overcomes the inconsistency of the classical theory, proposed in all books on centrifugal turbomachinery and based on the conservation of the angular momentum. More importantly, it was assessed that the new equation is significantly more accurate than the classical one in evaluating the outlet tangential velocity, a quantity which not only affects the diffuser performance, but also determines the inlet conditions for the volute. Using grid-converged, steady-state, RANS computations, the paper demonstrated that the application of the classical theory determines an average error of 13% in the estimation of the tangential velocity, whereas the new angular momentum equation gives the same quantity within an accuracy of 1.3 ~ 2.2%, depending on the turbulence model employed. Since the new angular momentum equation is still based on the assumption of steady two-dimensional flow, only steadystate simulations were considered, although the real flow inside a diffuser is unsteady (due to the impeller rotation). Similar results were obtained by considering a skewed inlet velocity profile (as usually occurs in a real compressor, where the diffuser inlet depends on the impeller outlet) demonstrating that the effectiveness of the proposed model is not affected by the employment of a more complex (and more realistic) inlet velocity profile. The accuracy of the model remains the same when analyzing the vaneless diffuser of a centrifugal pump.

The proposed model was also validated against experimental data of extensive test campaigns including both diffuser geometry and operating condition variations. The results show improved accuracy and precision with respect to the ideal case and 2.8% overall average deviation from measurements in terms of modulus of tangential velocity at the diffuser exit.

The numerical computations and experimental test have demonstrated that the new equation is capable of accurately modeling the angular momentum loss occurring in a vaneless radial diffuser, thus providing more accurate predictions of the outlet tangential velocity. For this reason, the new angular momentum equation can be effectively employed in the preliminary design or in the performance analysis of a vaneless radial diffuser. Given the explicit, non-iterative, single equation formulation of the model and the introduced simplifications, this can be regarded as a really noteworthy result: an accurate estimation of diffuser outlet conditions can easily be calculated by using a single thermodynamic loss parameter.

NOMENCLATURES

c	absolute velocity
c_u	tangential component of absolute velocity
D	Diameter
R	Radius
f	friction coefficient
F_r	friction correction according to Ludtke
$\dot{m}$	mass flow rate
Ma	absolute Mach number
p	static pressure
R'	gas constant
Re	Reynolds number
$s\%(\ )$	percentage deviation
S_d	diffuser surface
T	static temperature
u	impeller tangential velocity
z	axial coordinate
w	relative velocity
W_f	work done by friction forces

Greek

α	angle between absolute velocity and the tangential direction
γ	ratio of specific heats
δ	diffuser width
ΔAM	angular momentum loss
δ_{BL}	boundary-layer thickness
η_p	polytropic efficiency
ξ	wake coefficient
ν	kinematic viscosity
ρ	fluid density
τ_w	wall shear stress

https://doi.org/10.1017/jmech.2014.72 Published online by Cambridge University Press

Subscript

$_2$	diffuser inlet
$_3$	diffuser outlet
$_{CFD}$	value obtained by CFD simulation
$_{id}$	value obtained by the classical theory
$_{wf}$	value obtained from the proposed theory
$_0$	constant

Superscript

^{0}	total conditions
$\overline{val}$	average of the value

ACKNOWLEDGEMENTS

The authors would like to thank dear Luciano Andrea Catalano, who was Full Professor at the Department of Mechanical Engineering of the Polytechnic of Bari, for having inspired them to write this paper.

REFERENCES

1. Johnston, J. P. and Dean Jr, R. C., "Losses in Vaneless Diffusers of Centrifugal Compressors and Pumps: Analysis, Experiment, and Design," *Journal of Engineering for Power*, 88, pp. 49–60 (1966).
2. Bryans, A. C., "Diffuser for a Centrifugal Compressor," U.S. Patent No. 4,576,550. Washington, DC: U.S. Patent and Trademark Office (1986)
3. Nakagawa, K., Takagi, T., Abe, Y. and Sakai, H., "Diffuser for centrifugal Compressor," U.S. Patent No. 4,877,370. Washington, DC: U.S. Patent and Trademark Office (1989).
4. Arndt, N., Acosta, A. J., Brennen, C. E. and Caughey, T. K., "Experimental Investigation of Rotor-Stator Interaction in a Centrifugal Pump with Several Vaned Diffusers," *Journal of Turbomachinery*, **112**, pp. 98–108 (1990).
5. Dawes, W. N., "Simulation of the Unsteady Interaction of a Centrifugal Impeller with its Vaned Diffuser: Flow Analysis," *Transactions Journal of Turbomachinery*, 117, pp. 213–222 (1995).
6. Oh, H. W., Yoon, E. S. and Chung, M. K., "An Optimum Set of Loss Models for Performance Prediction of Centrifugal Compressors," *Proceedings of the Institution of Mechanical Engineers*, *Part A: Journal of Power and Energy*, **211**, pp. 331–338 (1997).
7. Hazby, H. R., Xu, L. and Schleer, M., "Study of the Flow in a Vaneless Diffuser at Part Speed Operating Conditions," *Proceedings of ASME Turbo Expo 2010: Powerfor Land, Sea and Air,* GT2010-22605, Glasgow, UK (2010).
8. Anish, S. and Sitaram, N., "Steady and Transient Computations of Intercation Effects in a Centrifugal Compressor with Different Type of Diffusers," *Proceedings of ASME Turbo Expo 2010: Power for Land, Sea and Air,* GT2010-22913, Glasgow, UK (2010).
9. Amirante, R., Catalano, L. A., Dadone, A. and Daloiso, V. S. E., "Design Optimization of the Intake of a Small-Scale Turbojet Engine," *Computer Modeling in Engineering and Sciences*, **18**, pp. 17–30 (2007).
10. Amirante, R., Catalano, L. A., Poloni, C. and Tamburrano, P., "Fluid-Dynamic Design Optimization of Hydraulic Proportional Directional Valves," *Engineering Optimization*, **46**, pp. 1295-1314 (2014).
11. Ferguson, T. B., *The Centrifugal Compressor Stage*, Butterworths, London (1963).
12. Lakshminarayana, B., *Fluid Dynamics and Heat Transfer of Turbomachinery*, John Wiley & Sons, Hoboken, New Jersey (1996).
13. Turton, R. K., *Principles of Turbomachinery*, Chapman and Hall Ltd., London (1984).
14. Gulich, H., *Centrifugal Pumps*, 2nd Edition, Springer, Berlin (2010).
15. Pfleiderer, C., *Kreiselpumpen für Flüssigkeiten und Gase*, Aufl, Springer, Berlin (1961).
16. Lüdtke, K. H., *Process Centrifugal Compressors*, Springer, Berlin (2004).
17. *FLUENT 6.3 User's Guide*, FLUENT INC. (2006).
18. Schlichting, H., *Boundary-Layer Theory*, McGraw Hill, New York (1968).
19. De Bellis, F., Grimaldi A., Rubino D. T., Amirante R. and Distaso E., "Accurate Vaneless Radial Diffuser 1-D Model with a Single Loss Parameter," *Proceedings of ASME Turbo Expo 2014: Turbine Technical Conference and Exposition*, GT2014-25232, Düsseldorf, Germany (2014).

(Manuscript received December 13, 2013,
accepted for publication May 23, 2014.)

https://doi.org/10.1017/jmech.2014.72 Published online by Cambridge University Press